铝锂合金填充式摩擦点焊微观组织演化

张成聪[1]， 封小松[1]， 郭立杰[1]， 左玉婷[2]
(1. 上海航天设备制造总厂 技术中心，上海 200245;
2. 北京有色金属研究总院 国家有色金属及电子材料测试中心，北京 100088)

摘 要: 利用光学显微镜、扫描电镜、电子背散射衍射(EBSD)等手段对5A90铝锂合金填充式摩擦点焊接头各个区域的微观组织进行了分析. 结果表明，焊核区发生完全动态再结晶，由细小的等轴晶组成，底部存在晶粒更加细小的细晶带，焊核区晶粒分布无明显织构. 热力影响区发生了部分再结晶，由发生再结晶的等轴晶以及发生部分回复的变形晶粒组成，具有较多的变形组织特征; 热力影响区与焊核区存在明显的分界面，分界面由尺寸明显小于周围晶粒的细晶组成，晶界较为密集.

关键词: 填充式摩擦点焊; 铝锂合金; 组织演化; 电子背散射衍射
中图分类号: TG 453 **文献标识码**: A **文章编号**: 0253-360X(2014)11-0075-04

0 序 言

填充式摩擦点焊(friction spot welding，FSpW)，是一项新型的点连接技术[1]. 其焊接过程包括摩擦预热阶段、下压搅拌阶段、材料回填阶段，焊后可获得无匙孔的光滑表面焊点. 相对于常见的点连接技术铆接和电阻点焊而言，填充式摩擦点焊具有减重、高效、绿色、高质量等优点，是轻金属合金最理想的点连接方法[2-4]. 同搅拌摩擦焊一样，填充式摩擦点焊是基于固相连接原理的焊接方法，在搅拌工具的摩擦和挤压作用下，材料发生剧烈的塑性变形并产生大量的热，温度升高，焊核区同时发生加工硬化和再结晶两个过程，对于接头最终的组织和性能有决定性影响.

目前对于填充式摩擦点焊的研究，大多集中在不同材料的可焊性上[5-9]，文中以铝锂合金为研究对象，对其接头不同位置微观组织的演化及动态再结晶行为进行了研究，研究结果将为深刻理解填充式摩擦点焊接头形成机理提供依据.

1 试验方法

试验材料为5A90铝锂合金板材，板厚1.5 mm，成分(质量分数，%)为4.5~6.0Mg，1.8~2.3Li，0.08~0.15Zr，Fe<0.2，Si<0.15，Ti<0.05，铝余量; 热处理状态为固溶+时效. 焊点接头沿直径截取制备金相试样，采用金相显微镜Axio Observer D1M观察焊点接头截面宏观和微观组织形貌. 采用HITACHII S-3400 N型扫描电子显微镜及其配置EBSD(电子背散射衍射)系统对接头组织形貌进行分析. EBSD试样经机械抛光以后进行电解抛光，抛光液为1.8%的氟硼酸，抛光时间20 s，抛光电压30 V，抛光液温度20 ℃. 对电解抛光好的样品进行EBSD测试，测试电压20 kV.

收稿日期: 2013-06-16
基金项目: 国防基础科研项目资助(A0320110014)

2 试验结果与分析

在填充式摩擦点焊过程中，搅拌工具旋转和相对运动，摩擦和挤压材料，母材发生了动态再结晶，其微观组织发生了变化. 图1给出了铝锂合金摩擦点焊接头的宏观组织，按其组织特征，可分为母材(BM)、热力影响区(TMAZ)、焊核区(NZ). 对不同区域的组织特征和演化过程进行了分析.

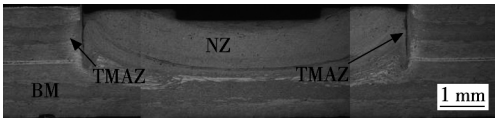

图1 点焊接头典型宏观组织
Fig. 1 Cross-section of typical spot weld

2.1 母材的组织特征分析

为了分析母材的组织特征，采用EBSD的方法对母材200 μm×150 μm的区域样品进行了分析，

步长 0.5 μm. 图 2a 为该区域的 IQ(image quality) 图以及大小角度晶界的分布,可以看出,该区域晶粒沿着加工方向拉长成长条状,且晶粒沿宽度方向的尺寸约为几到十几微米,大部分晶粒内部存在大量的 2° ~ 15°小角度晶界. 图 2b 为取向成像图,可以看出,大量的晶粒都具有相近的颜色,表明该扫描区域内晶粒存在明显的择优取向,即织构. 用 OIM Analysis 软件计算了母材中的极图及 ODF(orientation distribution function) 图,并计算出各织构的百分数,结果如图 3 所示.

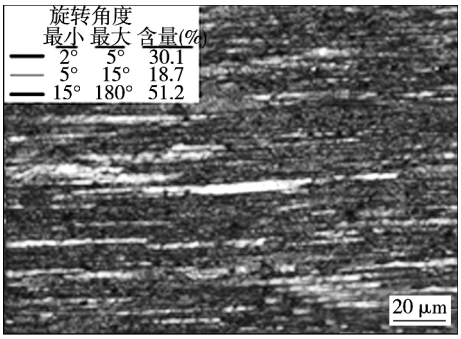

(a) IQ图与大小角度晶界分布

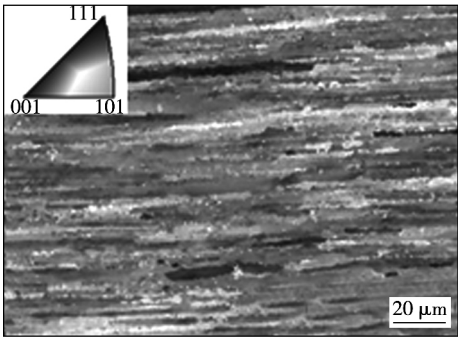

(b) 取向成像图

图 2 母材微观组织分析

Fig. 2 Microstructure feature of base material

从极图及 ODF 图中可知,极图的极密度最大值为 12.17,ODF 图中极密度最大值为 35.2,说明母材中存在较强的织构. 从{111}极图中可以看出,母材存在较强的 S 织构{123} <634>,以及黄铜织构{110} <112>,同时还有 R 织构{124} <211>,经计算,S 织构为 30.5%,黄铜织构含量为 23.3%,R 织构为 26%.

2.2 焊核区微观组织分析

为了深入分析焊缝中心的组织特征,对焊缝中心区域进行了 EBSD 分析,分析区域大小为 300 μm ×200 μm,步长为 0.8 μm. 图 4 为该区域的组织重构图. 从图 4a 可以看出,该区域主要由尺寸约 10 μm 的等轴晶粒组成,晶粒尺寸较均匀. 从图 4b 取向成像图中没有看出该区域存在明显的织构.

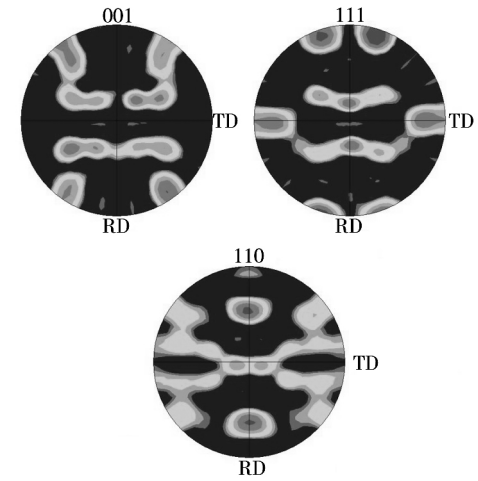

(a) {001},{110},{111}极图

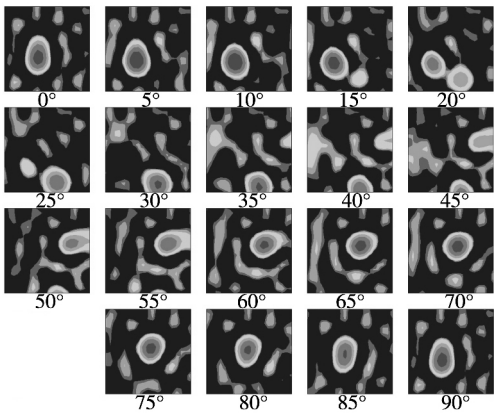

(b) ODF图

图 3 母材极图与 ODF 图

Fig. 3 Pole figure and ODF figure of base material

同时观察发现,焊核区底部的晶粒尺寸较小,存在一条明显的细晶带,晶粒内部小角度晶界明显更多. 由分析可知,在搅拌套下压的过程中,底部材料被挤入搅拌针上升留下的空间,进而被挤出,经历了较大的塑性变形,具有高的应变速率,因此其再结晶的形核率较高,易产生细晶组织. 另外,由于焊核底部的材料靠近垫板,散热较快,其变形温度较低,使得再结晶晶核长大受阻,因此底部保留了细晶带.

为了与母材原始组织对比,计算了焊核区的极图及 ODF 图(图 5) ,分析焊缝中心织构. 从图 5 可知,极图与 ODF 最大极密度值分别为 1.927,2.73,焊缝中心区域织构较弱. 在摩擦点焊过程中,存在明显织构的母材组织消失,由动态再结晶形成的细小等轴晶替代,晶粒杂乱排列,没有明显的择优取向,即无明显织构.

与 FSpW 不同的是,FSW 的焊核区存在较为复杂的织构[10],主要是因为 FSW 是一个连续的准稳态过程,焊核区材料在焊接过程中经历了动态再结

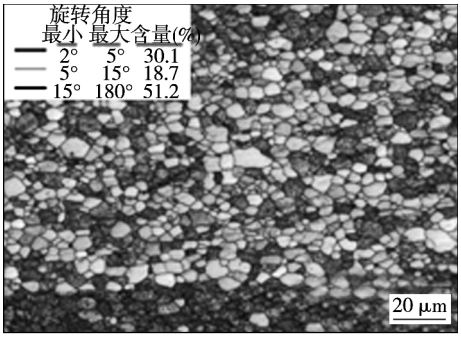

(a) IQ图与大小角度晶界分布

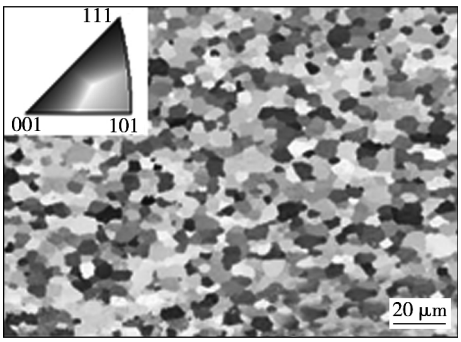

(b) 取向成像图

图 4　焊核区微观组织分析

Fig. 4　Microstructure feature of nugget

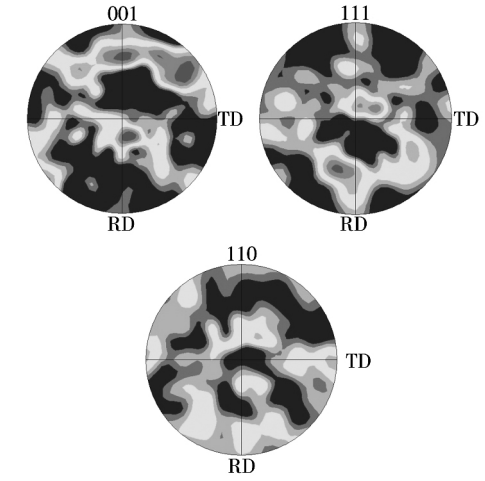

(a) {001},{110},{111}极图

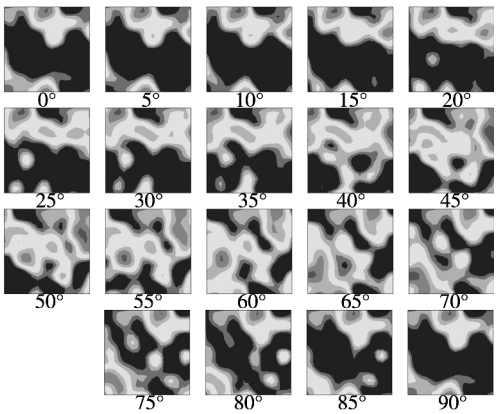

(b) ODF图

图 5　焊核区极图与 ODF 图

Fig. 5　Pole figure and ODF figure of the nugget

晶、二次变形等复杂的周期性变化，使得焊缝处晶粒形成了较为复杂的择优取向. 而 FSpW 是针对局部材料的单次作用，材料流动较为简单，经历了较为单一的动态再结晶行为，因此其焊核区未产生明显织构.

2.3　热力影响区组织特征分析

为了深入分析热力影响区晶粒组织特征，对该区域进行了 EBSD 分析(图 6)，分析区域大小为 250 μm × 150 μm，步长为 0.5 μm.

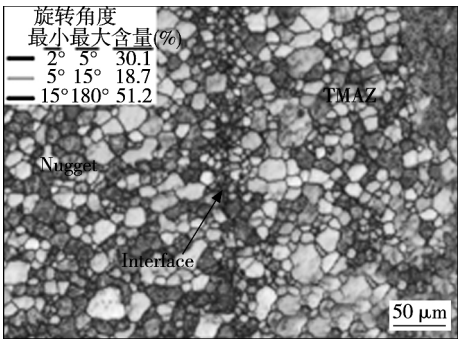

图 6　热力影响区微观组织

Fig. 6　Microstructure feature of TMAZ

图 6 中左侧为焊核区的等轴细晶组织，右侧为热力影响区组织，晶粒内部存在大量 2° ~ 15°的小角度晶界；紧邻焊缝中心的热力影响区发生了较大程度的再结晶，靠近母材处则主要发生了回复及晶粒长大.

从母材到焊核区，热力影响区再结晶程度逐渐增大，其组织特征变化代表了材料在焊接过程中的组织演化过程. 靠近母材一侧的变形组织中存在大量的小角度晶界，这些小角度晶界吸收位错，使其取向差增加而变成大角度晶界，从而形成焊核中的等轴晶组织. 这种小角度晶界不断吸收位错而使取向差增加，最终转变成大角度晶界的机制称为连续动态再结晶[11,12]，这一特征与 FSW 类似.

从图 6 中可以看出，分界面由尺寸明显小于周围晶粒的细晶组织组成，晶界较为密集. 在焊接过程中，由于搅拌套的旋转下压，使材料发生分离，在随后的冷却过程中，材料在高温区停留的时间较短，再结晶晶粒的晶界迁移受到阻碍，细小晶粒来不及长大而保留下来. 这种不均匀组织所形成的界面可能在受载过程中成为整个接头的弱连接而首先产生裂纹断裂.

3　结　　论

(1) 在焊接的热、力作用下，焊核区发生完全动态再结晶，产生细小的等轴晶，底部存在晶粒更加细

小的细晶带;焊核区无明显织构.

(2) 热力影响区发生了部分再结晶,由发生再结晶的等轴晶以及发生部分回复的变形晶粒组成,保留了较多的变形组织特征.

(3) 热力影响区与焊核区存在明显的分界面,分界面由尺寸明显小于周围晶粒的细晶组成,晶界较为密集.

参考文献:

[1] Schilling C, Dos Santos J F. Method and device for linking at least two adjoining work pieces by friction welding [P]. European patent EP 1230062 B1 (WO 2001/036144); 1999.

[2] 赵衍华,张丽娜. 搅拌摩擦点焊技术简介 [J]. 航天制造技术,2009,(2): 1-5.
Zhao Yanhua, Zhang Lina. Introduction of friction stir spot welding technology [J]. Aerospace Manufacturing Technology, 2009, (2): 1-5.

[3] 张 健,董春林. 搅拌摩擦点焊在航空领域的应用 [J]. 航空制造技术,2009,(16):70-73.
Zhang Jian, Dong Chunlin. Application of friction stir spot welding in aviation industry [J]. Aeronautical Manufacturing Technology [J], 2009,(16):70-73.

[4] Silva A A M, Dos Santos J F, Rosendo T, *et al*. Friction spot and friction stir spot welding processes-a literature review [J]. Bull Natl R&D Inst Weld Mater Test BID/ISIM, 2007, 16: 36-44.

[5] Rosendo T, Tier M A D, Ramos F D, *et al*. Preliminary investigations on microstructural and mechanical properties of friction spot welding of 2 mm-thick AA2024 T3 aluminium alloy [C] // In: IIW international congress 2nd Latin American welding congress XXXIV Consolda, National Welding Congress, Sao Paulo, Brasil; 2008.

[6] Rosenda T, Parra B, Tier M A D, *et al*. Mechanical and microstructual investigation of friction spot welded AA6181-T4 aluminium alloy [J]. Materials & Dsign, 2011, 32(3): 1094-1100.

[7] Amancio-Filho S T, Bueno C, Dos Santos J F, *et al*. On the feasibility of friction spot joining in magnesium/fiber-reinforced polymer composite hybrid structures [J]. Materials Science and Engineering A, 2011, 528: 3841-3848.

[8] Oliveira P H F, Amancio-Filho S T, Dos Snatos J F, *et al*. Preliminary study on the feasibility of friction spot welding in PMMA [J]. Materials Letters, 2010, 64: 2098-2101.

[9] Campanelli L C, Suhuddin U F H, dos Santos J F. Preliminary investigation on friction spot welding of AZ31 magnesium alloy [J]. Materials Sciense Forum, 2012, 709(4): 3016-3021.

[10] Mishra R S, Ma Z Y. Friction stir welding and processing [R]. Materials Science and Engineering: R: Reports, 2005, 1-78.

[11] Arora K S, Pandey S, Schaper M, *et al*. Microstructure evolution during friction stir welding of aluminum alloy AA2219 [J]. Journal of Material Science and Technology, 2010, 26(8): 747-753.

[12] 张成聪,常保华,陶 军,等. 2024 铝合金搅拌摩擦焊过程组织演化分析 [J]. 焊接学报,2013,34(3): 57-60.
Zhang Chengcong, Chang Baohua, Tao Jun, *et al*. Study on the microstructure evolution during friction stir welding of 2024 aluminum alloy [J]. Transactions of the China Welding Institution, 2013, 34(3): 57-60.

作者简介: 张成聪,男,1986 年出生,硕士研究生. 主要从事航天用固相连接技术、微连接技术方面的研究工作. 发表论文 5 篇. Email: zhangcc0202@163.com

通讯作者: 封小松,男,高级工程师. Email: fxsupc@nuaa.edu.cn

[上接第 74 页]

friction stir welding [J]. Hot Wording Technology, 2010, 39(19): 156-158.

[11] 赵华夏,董春林,栾国红. 搅拌摩擦焊接头形成过程分析 [J]. 焊接学报,2012,33(12): 93-96.
Zhao Huaxia, Dong Chunlin, Luan Guohong. Forming process study of friction stir welding joint [J]. Transactions of the China Welding Institution, 2012, 33(12): 93-96.

作者简介: 赵华夏,男,1980 年出生,博士,高级工程师. 主要从事搅拌摩擦焊接机理及工艺研究. 发表论文 11 篇. Email: zhhq@sina.com

tion results showed that horizontal clamping gap had greater influence on welding spot than vertical clamping gap, and the maximum stress at each single welding spot reduced with the increasing of welding spots quantity and effective connection area.

Key words: spot welding; welding deviation; stress and strain

Process and performance of cold metal transfer spot plug welding between aluminum alloy and bare steel HUANG Qian[1], CAO Rui[1], ZHU Haixia[1], CHEN Jianhong[1], WANG Peichung[2] (1. State Key Laboratory of Advanced Processing and Recycling of Non-ferrous Metals, Lanzhou University of Technology, Lanzhou 730050, China; 2. GM R&D Center, Warren MI 48090, USA). pp 59 - 62

Abstract: Cold metal transfer (CMT) spot plug welding of Al6061 and bare steel was carried out by using $AlSi_5$ filler metal. Using orthogonal test method to optimize process parameters, the microstructure and mechanical properties of welded joint were investigated with optical microscope, scanning electron microscopy and universal tensile testing machine. The results show that the welded joint between Al6061 and bare steel could obtain satisfied weld appearance and performance using CMT method. The sequence of significance of process parameters was hole size in bare steel sheet, spot welding time and wire feed speed. The results also indicated that the typical spot welding-brazing joint, which consisted of brazing zone and the welding zone, could be performed; the pore was the main defect in the welded joint; the maximum shear strength of the joint was more than 4 kN with tear fracture.

Key words: cold metal transfer spot plug welding; Al/bare steel sheet; orthogonal test; mechanical property

Effect of hygrothermal environment on microstructure and mechanical properties of Zn-2Al filler metal LÜ Dengfeng[1], LONG Weimin[1], ZHANG Guanxing[1], WANG Xingxing[1], HE Peng[2] (1. State Key Laboratory of Advanced Brazing Filler Metals & Technology, Zhengzhou Research Institute of Mechanical Engineering, Zhengzhou 450001, China; 2. State Key Laboratory of Advanced Welding and Joining, Harbin Institute of Technology, Harbin 150001, China). pp 63 - 66

Abstract: The aging degradation behavior of Zn-2Al filler metal in hot and humid environment was studied. High temperature and high humidity accelerating test was conducted to simulate the hygrothermal atmospheric corrosion condition. The influence of corroding time on the microstructure, mechanical properties and wettability of Zn-2Al filler metal was investigated. The experimental results displayed linear relationship between corroding depth and corroding time. Water vapor corroding primarily occurred at grain boundaries, and when corrosion reached a certain extent, corrosion cracks and corrosion holes formed. This intergranular corrosion was electrochemical corrosion with the intragranular zinc-rich η phase as the cathode but the aluminum-rich α phase as the anode that dissolute at grain boundary. The tensile strength, plasticity and toughness of Zn-2Al filler metal decreased, and the wetting area of Zn-2Al filler metal on 1060 aluminum sheet also decreased sharply with the increase of corroding time.

Key words: Zn-Al filler metal; hygrothermal environment; intergranular corrosion; mechanical properies; microstructure

Effect of salt spray environment on mechanical properties of aluminum welded joints treated with ultrasonic impact LI Da[1], WANG Xiaomin[2], SUN Bing[1], CHEN Hui[1], LIU Liyun[1], LI Peng[3] (1. College of Material Science and Engineering, Southwest Jiaotong University, Chengdu 610031, China; 2. College of Life Science and Engineering, Southwest Jiaotong University, Chengdu 610031, China; 3. CSR SIFANG CO., LTD., Qingdao 266111, China). pp 67 - 70

Abstract: The Al6005 welded joint was treated with ultrasonic impact and the residual stress of the treated and untreated specimens was measured. The results showed that uniform compressive stress distributed in the weld and heat-affected zone (HAZ) after the joint was treated with ultrasonic impact. The properties of welded joint were discussed after salt spray corrosion test. The results indicated that the treated joint produced less corrosion product after corrosion for different times. The hardness of the weld metal and HAZ increased after the joint was treated with ultrasonic impact. The thickness of hardened layer in the weld metal and HAZ was 1.5 mm and 2.1 mm, respectively. The thickness of hardened layer maintained at 0.9 mm after corrosion for 14 days. Besides, the welded joint after treatment could have better mechanical properties than untreated joints.

Key words: aluminum welded joints; ultrasonic impact; salt spray corrosion; residual stress; mechanical property

Section contour analysis of probe during friction stir welding ZHAO Huaxia, MENG Qiang, DONG Jihong, DONG Chunlin, LUAN Guohong (Beijing Aeronautical Manufacturing Technology Research Institute, Aviation Industry Corporation of China, Beijing 100024, China). pp 71 - 74, 78

Abstract: Based on the section analysis of three-dimensional model of friction stir welding, the moving expressions about feature points on section contour of probe were established. According to the basis of mathematical analysis, the forming mechanisms of hook, cold overlap-defect and onion structure were revealed. In the light of the above research results, the optimization idea of probe shape was proposed. Considering improving plastic metal migration behavior, the s-line of large thickness aluminum alloy friction stir welded butt joint and cold overlap-defect in lap joint of stringer and plate was effectively eliminated by three aspects design. The results provide technical support for the development of friction stir welded products.

Key words: friction stir welding; section analysis; hook; cold overlap-defect

Microstructure evolution during refill friction spot welding of aluminium-lithium alloy ZHANG Chengcong[1], FENG Xiaosong[1], GUO Lijie[1], ZUO Yuting[2] (1. Technical Center, Shanghai Aerospace Equipments Manufacturer, Shanghai 200245, China; 2. National Center of Analysis for Nonferrous

Metal and Electronic Material, General Research Institute for Nonferrous Metals, Beijing 100088, China). pp 75 – 78

Abstract: The optical microscope, scanning electron microscope (SEM) and electron back scattered diffraction (EBSD) were used to analyze the microstructure in different reigns of refill friction spot welded (RFSW) joints. The results showed that complete dynamic recrystallization occurred in the nugget zone with fine equiaxial grains, and much finer grains existed at the bottom. The nugget zone had no obvious texture. Part dynamic recrystallization occurred in the TMAZ which contained fine equiaxial grains and partly recovery grains with deformed structure. An obvious interface existed between the nugget zone and TMAZ, and its grain was much finer than those on both sides, and the grain boundary was denser.

Key words: refill friction spot welding; aluminium-lithium alloy; microstructure evolution; electron back scattered diffraction

Microstructure evolution after thermal exposure in weld interface of Ti_2AlNb/TC11 dual alloy forged at different temperatures JIA Qian[1,2], YAO Zekun[1,2], ZHANG Dongya[1,2], QIN Chun[1,2], TU Weijian[1,2], YANG Guobao[1,2], GENG Jingdong[3] (1. College of Materials Science and Engineering, Northwestern Polytechnical University, Xi'an 710072, China; 2. ERC of Forging Technique for Less Deformable Materials, Xi'an 710072, China; 3. Blade Factory of Guizhou Aero-Power Company, Pingba 561114, China). pp 79 – 83

Abstract: The microstructure evolution in Ti2AlNb/TC11 dual alloys after near thermal forging, gradient heat treatment and thermal exposure at 550 ℃ for 50 h and 100 h, respectively, was investigated with optical microscope (OM) and transmission electron microscope (TEM). The results show that B2→O + β decomposition occurred in the welded seam and Ti_2AlNb matrix, and α_2 phase migrated to the grain boundary of B2 during thermal exposure. The time for thermal exposure was longer, the segregation of α_2 phase at grain boundary was severer. And α_2 phase agglomerated into block when the thermal exposure time was 100 h. Also, the β phase grew coarse and its volume percentage increased simultaneously. If Al and Nb contents were large in the joint, α_2 phase would agglomerate at grain boundary, the original O phase overprinting with the secondary O phase decomposed from B2 phase would coarsen.

Key words: dual alloys; near thermal forging; thermal exposure; microstructure

Influence of weld strength match on distribution of stress triaxiality for aluminum alloy welded joint ZHU Hao[1,2], GUO Zhu[1,2], CUI Shaopeng[1,2], WANG Yanhong[1,2] (1. Hebei Provincial Key Laboratory of Traffic Engineering materials, Shijiazhuang TieDao University, Shijazhuang 050043, China; 2. School of Materials Science and Engineering, Shijiazhuang TieDao University, Shijazhuang 050043, China). pp 84 – 88

Abstract: The tensile simulation was carried out on 6063 aluminum alloy welded joint with different weld strength matches with software ABAQUS, and the influence of weld strength match on the distribution of stress triaxiality in aluminum alloy welded joint was studied. At the same time, the influence of HAZ width on the distribution of stress triaxiality in welded joint was studied in each strength match condition. The results indicate that the stress state in welded joints with different weld strength matches was complicated, compared to the base material. Bounce in the stress traxiality existed in the boundary between the base material and HAZ and between the weld and HAZ. The maximum of stress traxiality in high strength match welded joint was the largest. On the contrary, the maximum of stress traxiality in low strength match welded joint was the least. Under the condition of equal strength match, the position of the maximal stress traxiality changed from the boundary between the base material and HAZ to the boundary between the weld and HAZ with the increasing of the width of HAZ. Under the condition of high strength match, the maximum of stress traxiality appeared in the boundary between the weld and HAZ, and the maximum of stress traxiality reduced gradually with the increasing of the width of HAZ. However, under the condition of low strength match, the maximum of stress traxiality appeared in the boundary between the base material and HAZ, and the maximum of stress traxiality also reduced gradually with the increasing of the width of HAZ.

Key words: aluminum alloy welded joint; strength match; HAZ; stress triaxiality; FEA

A control technique for electron-beam scan welding WEI Shouqi, LI Xuejiao, MO Jinhai (College of Mechanical & Electrical Engineering, Guilin University of Electronic Technology, Guilin 541004, China). pp 89 – 92, 96

Abstract: In electron-beam (EB) scan welding, the 2D seam tracking could be approximated by combination of limited line segments and basic arc graphics, hence the whole welding processes could be divided into 3 steps: tracing of teaching, calculating of tracking data, and scan welding. In these processes, three main problems, non-vertical of x-y scanning axis, distortion of scanning track and defocusing of EB spot could be solved by proper conversion of oblique and rectangular coordinates, dynamic correction of deflection scanning magnetizing current with EB's deflection amplitude and velocity, and dynamic correction of focusing magnetizing current with EB's deflection vector, respectively. The welding results with "track & field" type seam tracking reveal that, eccentric distance is above 0.08 mm, depth error is lower than 0.13 mm, width error in surface is lower than 0.16 mm. The proposed welding method could precisely repeat the seam tracking and obtain excellent welding quality.

Key words: electron-beam scan welding; coordinate conversion; scanning track distortion; electron-beam spot defocusing

Test and analysis on corrosion resistance of MWEDM surfaces ZHANG Bin[1,2], GUO Libin[1], CUI Hai[1,3], ZHANG Huigang[1] (1. College of Mechanical and Electrical Engineering, Harbin Engineering University, Harbin 150001, China; 2. Library, Harbin Engineering University, Harbin 150001, China; 3. Engineering Training Center, Harbin Engineering University, Harbin 150001, China). pp 93 – 96